DETERMINATION OF EFFECTIVE COEFFICIENT OF CHINESE FIR (*CUNNINGHAMIA LANCEOLATA*) DURING ADSORPTION AND DESORPTION PROCESS

Yuxin Wen

PhD Student
School of Technology
Beijing Forestry University
Beijing 100083, P.R. China
E-mail: when0714@bjfu.edu.cn

Ping Yang

Researcher
Beijing Institute of Science and Technology Information
Beijing 100083, P.R. China
E-mail: yangping1989@163.com

Jian Zhao

Associate Professor
E-mail: zhaojian1987@bjfu.edu.cn

*Dong Zhao**

Professor
School of Technology
Beijing Forestry University
Beijing 100083, P.R. China
E-mail: zhaodong68@bjfu.edu.cn

(Received March 2019)

Abstract. Establishing an accurate moisture transport model in wood is essential to analyze the hygroscopic behavior and estimate the stability of wood structures in the ambient environment. In this article, the effective diffusion coefficients (EDCs) of Chinese fir in radial and tangential directions during adsorption and desorption processes were measured based on the differential model, and numerical simulations were performed to verify the rationality of measured results. The results show that 1) for adsorption process, the surface emission coefficient (SEC) and EDC of Chinese fir are all greater in the radial direction; 2) for desorption process, the SEC is higher in the radial directions, whereas the EDC in the tangential direction is higher than that in the radial direction when the MC is greater than 10%; 3) the SEC and EDC in the adsorption process are larger than those in the desorption process. Because there is a reasonable agreement between experimental and numerical simulation results, the measured results could be used to predict the MC distribution of Chinese fir in the ambient environment.

Keywords: Adsorption, Chinese fir, desorption, effective diffusion coefficient (EDC), surface emission coefficient (SEC), moisture content (MC).

INTRODUCTION

Chinese fir (*Cunninghamia lanceolata*) is one of the most important economic wood species in China which is widely applied in construction and wood working industry. As a hygroscopic material likes other wood materials, Chinese fir lumber can exchange water molecules with the ambient environment on the surface, then the MC of it varies gradually and tends to close to equilibrium with the air humidity (Ma et al 2005; Niklewski et al 2016). With the variations of RH

* Corresponding author

Wood and Fiber Science, 51(4), 2019, pp. 364-374
https://doi.org/10.22382/wfs-2019-035

in the environment, the induced moisture gradients will lead to moisture-induced stresses rise. When the moisture-induced stress exceeds the strength of wood, cracks may develop, which would cause timber structures to fail (Angst and Malo 2012).

On the other hand, the variation of MC can also significantly affect the properties of wood (Kollmann and Cote 1968). When being absorbed on the surface of microfibers, water molecules in the cell walls of wood will replace the hydrogen bonds in the fibers and then cause the stiffness of wood to decrease because of the effects of plasticizer (Zhan et al 2015). As a result, mechanical and physical property parameters of wood, such as modulus of elasticity, yield and ultimate stress values, creep response, creep compliance, and fluidity in stress relaxation process, will be varied obviously with the increase in MC, which would cause the moisture-induced stress to increase more sharply (Roszyk et al 2012; Zhao et al 2012; Kaboorani et al 2013; Zhan et al 2015; Jiang et al 2017). Thus, an accurate moisture transport model to predict the development and distribution of moisture in wood is a key for estimating the stability and service life of timber structures.

Skaar (1988) developed a diffusion model based on Fick's second law to simulate the moisture transfer process in wood. Even some recent studies indicated there are some deviations on the diffusion models based on Fick's second law because of non-Fickian sorption (Crank 1986; Wadso 1993; Shi 2007), but this diffusion model still provided successful predictions for moisture movements and moisture-induced stresses during adsorption and desorption process in wood (Sundström et al 2011; Angst and Malo 2013; Salinas et al 2015; Niklewski et al 2016). The diffusion model is expressed as follows:

$$\frac{\partial M}{\partial t} = \frac{\partial}{\partial x}\left(D \cdot \frac{\partial M}{\partial x}\right), \tag{1}$$

where M is the MC, t is the time, and D is the effective diffusion coefficient (EDC, unit: $m^2\ s^{-1}$). When the MC is less than the FSP, the value of EDC can be illustrated by an exponential-type function (Hukka 1999); see Eq 2:

$$D = \exp(\alpha + \beta M). \tag{2}$$

The initial and boundary conditions are given by Eq 3:

$$\begin{cases} M = M_0 \ \text{ for } \ t = 0 \ \text{ (Initial)} \\ D \cdot \nabla M = S\left(M_{\text{eq}} - M_{\text{surf}}\right) \text{ for flux boundary} \\ D \cdot \nabla M = 0 \ \text{ for boundarty without flux,} \end{cases} \tag{3}$$

where M_0 is the initial MC of wood, M_{surf} is the MC at the surface of the wood, S is the surface emission coefficient (SEC, unit: $m \cdot s^{-1}$), and M_{eq} is the EMC. Based on the Wood Handbook published by USDA (2010), the values of EMC under different temperature and RH can be calculated by Eq 4:

$$M_{\text{eq}} = \frac{18}{W}\left[\frac{Kh}{1-Kh} + \frac{K_1Kh + 2K_1K_2K^2h^2}{1 + K_1Kh + K_1K_2K^2h^2}\right], \tag{4}$$

where h is the RH and W, K, K_1, and K_2 are parameters depending on temperature:

$$\begin{aligned} W &= 349 + 1.29T + 0.0135T^2 \\ K &= 0.805 + 0.000736T - 0.00000273T^2 \\ K_1 &= 6.27 - 0.00938T - 0.000303T^2 \\ K_2 &= 1.91 + 0.0407T - 0.000293T^2, \end{aligned}$$

where T is temperature (units: °C).

Previous research studies on parameters in the diffusion model showed that the values of diffusion parameters are correlated with wood species (Simpson 1974; Chen et al 1996; Eriksson et al 2006; Gatica et al 2011, 2012; Salinas et al 2015). For softwoods such as Chinese fir, the elementary fibrils in the microfibrils are arranged more loosely and disorderly than hardwood, which leads to a faster diffusion process in softwood Tsuchikawa and Siesler (2003a, 2003b). However, few of them separated differences between radial and tangential values of internal moisture diffusion. Yeo et al

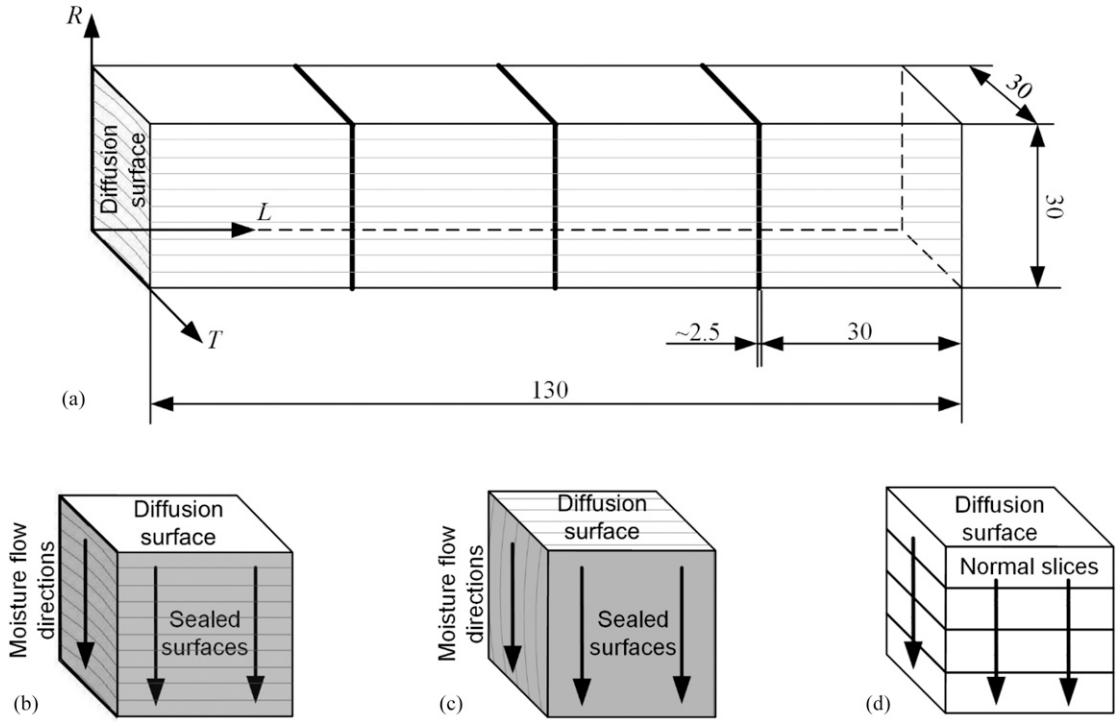

Figure 1. Test samples. (a) Chinese fir stick cut off from freshly sawn timber, (b) radial and (c) tangential diffusion samples, and (d) samples sectioned into four normal slices.

(2008) noted that the internal moisture movement rate in each orientation is quite different, which indicated that a more accurate diffusion model separating moisture transport in different directions is needed. Besides, the existence of pore diffusion (Nakano 1995; Shi 2007) and nonequilibrium excess number of sorption sites (Willems 2014) could also cause moisture-transporting behaviors to be different during adsorption and desorption process. Ma et al (2005) also investigated the sorption behaviors of Chinese fir at nonequilibrium state and observed that isothermal adsorption curve lies below the desorption curve, known as the phenomenon of sorption hysteresis. Therefore, identifying the diffusion parameters in different orthogonal directions and different sorption process is crucial for predicting moisture and material behavior of Chinese fir.

In this article, based on Fick's second law and the finite volume method, the diffusion parameters of Chinese fir on radial and tangential directions were determined by adsorption and desorption experiments using the differential model proposed by Gatica et al (2011, 2012). This model offered a simple method with low computational cost to determine the diffusion parameters in the

Table 1. Samples in determination experiments for effective diffusion coefficient and surface emission coefficient.

Samples	Experiments	Flux surface	Moisture flow direction	Initial MC (%)	Environmental parameters
Radial adsorption	Adsorption	TL	R	0	25°C, RH = 85%
Tangential adsorption	Adsorption	RL	T	0	25°C, RH = 85%
Radial desorption	Desorption	TL	R	17.8	25°C, RH = 50%
Tangential desorption	Desorption	RL	T	17.8	25°C, RH = 50%

TL, tangential-longitudinal; RL, radial-tangential.

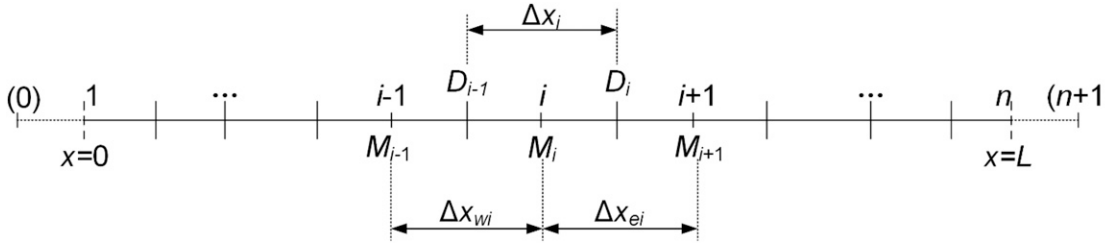

Figure 2. Discretization scheme of variables for the mathematical model.

isothermal drying process with a higher accuracy. Then, numerical simulation experiments were performed by the finite element method to verify the rationality of measured results. This study will provide proofs for developing an accurate moisture transport model of wood during adsorption and desorption processes and estimating the stability of timber structures in the ambient environment.

MATERIALS AND METHODS

Moisture Diffusion Experiments

In this study, a 2-m long freshly sawn timber was cut at the breast height of a 20-yr-old Chinese fir (*C. lanceolata*) from Quanzhou, China. The timber was first cut off into four 130-mm-long sticks with a cross-sectional dimension of 30 × 30 mm^2 (radial × tangential, $R \times T$). Then the stick was cut into four parts with dimensions of 30 × 30 × 30 mm^3 (longitudinal × radial × tangential, $L \times R \times T$). All these specimens were free from defects, and edges of them were oriented in the typical orthotropic directions, see Fig 1(a). These specimens were randomly divided into four groups: radial adsorption (WR), radial desorption (DR), tangential adsorption (WT), and tangential desorption (DT), and each group contained four samples (Samples 1-4), see Table 1 and Fig 1(b) and (c). Except one of the diffusion surfaces, all the surfaces of each samples were covered with silicone glue.

Determination experiments of EDC and SEC contained moisture adsorption and desorption experiments. Before the experiments were performed, all the samples were absolutely dried in a drying box (Haowei WGL101-2A, Hebei, China) with the temperature of 103 ± 2°C and the mass was measured every 2 h using a precision balance (accuracy 0.01 g) until reached constant. Specially, for desorption experiments, the samples were then placed in a climate chamber (Zhongxing HWS-150, Beijing, China) with an RH of 85% and a temperature of 25°C for 2 wk until reached the initial MC.

The experiments were performed using the climate-controlled chamber (HWS-150), which can maintain the test conditions (plotted in Table 1) automatically. Mass of each sample was measured and recorded every 24 h using a precision balance (accuracy 0.01 g) to determine the MC.

For adsorption experiments, samples in each group (WR1 to WR4 and WT1 to WT4) were respectively sectioned into four normal slices

Table 2. Determination of algebraic symbols in Eq 7.

Algebraic symbol	$i=n$	$2 \le i \le n-1$	$i=1$
a_{wi}	$-\dfrac{D_{wn}}{\Delta x_{wn}}$	$-\dfrac{D_{wi}}{\Delta x_{wi}}$	0
a_{ei}	0	$-\dfrac{D_{ei}}{\Delta x_{ei}}$	$-\dfrac{D_{e1}}{\Delta x_{e1}}$
a_{ti}	$\dfrac{\Delta x_{wi}+\Delta x_{ei}}{2\Delta t}$	$\dfrac{\Delta x_{wi}+\Delta x_{ei}}{2\Delta t}$	$\dfrac{\Delta x_{wi}+\Delta x_{ei}}{2\Delta t}$
a_i	$-a_{wn}+S+a_{tn}$	$-(a_{wi}+a_{ei})+a_{ti}$	$-a_{e1}+a_{t1}$
b_i	$a_{tn}M_n^0+SM_{\mathrm{eq}}$	$a_{ti}M_i^0$	$a_{t1}M_1^0$

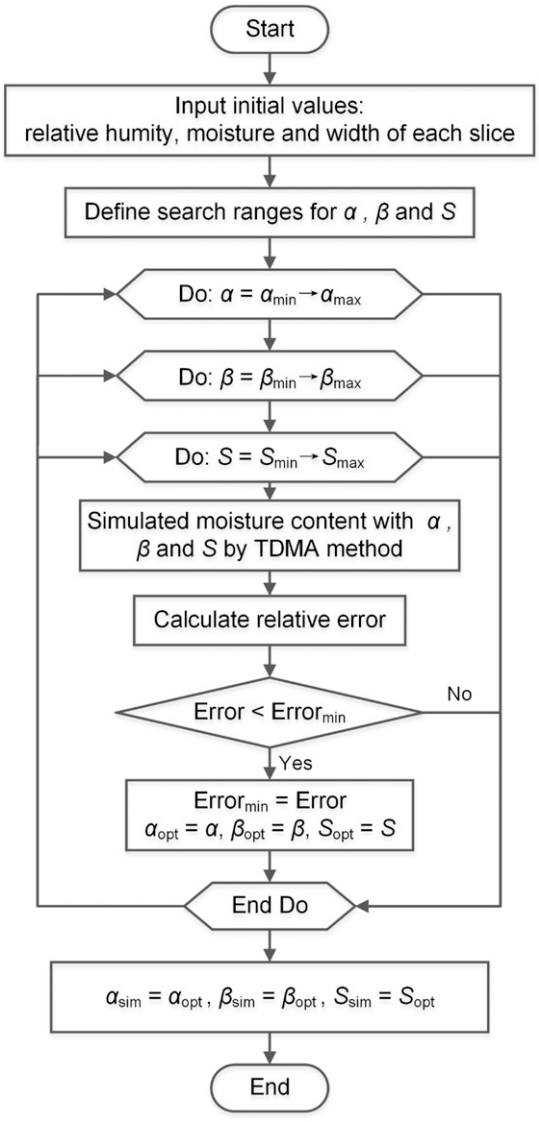

Figure 3. Flowchart of the tridiagonal matrix algorithm used to determine the optimum values of parameters.

along the moisture flow direction (see Fig 1(d)) at an MC of 8%, 10%, 12%, and 14%. For desorption experiments, samples in each group (DR1 to DR4 and DT1 to DT4) were sectioned into four normal slices along the moisture flow direction (see Fig 1(d)) when the MC reached 14%, 12%, 10%, and EMC (approximately 9.1%).

After all the experiments were finished, the MC of each slice was determined after being absolutely dried in the drying box. Then, the values of EDC and SEC on radial and tangential directions in adsorption and desorption processes can be computed based on the mathematical model.

Mathematical Model

The EDC and SEC of wood can be determined with the mathematical model suggested by Gatica et al (2011). In this differential model, the domain on the moisture flow direction $0 \le x \le L$ is subdivided into n subdomains based on the finite volume method, see Fig 2. Water is diffused from the section of $x = L$ to $x = 0$; thus, MC of the subdomain $i\,(1 \le i \le n)$ is varied from M_i^0 (initial MC) to M_i (final MC). Based on the finite volume model shown in Fig 2, Fick's second law can be translated into Euler fully implicit scheme by the rule of the middle point:

$$\frac{M_i - M_i^0}{\Delta t} = \left[\left(D_i \frac{M_{i+1} - M_i}{\Delta x_{ei}}\right) - \left(D_{i-1} \frac{M_i - M_{i-1}}{\Delta x_{wi}}\right)\right] \Big/ \Delta x_i, \tag{5}$$

where Δx_i is the width of the subdomain i, D_i is the EDC of the subdomain i in the initial time, Δx_{wi} is the distance between subdomain $i-1$ (west subdomain) and i, and Δx_{ei} is the distance between subdomain i and $i+1$ (east subdomain). The value of Δx_{wi} and Δx_{ei} can be calculated as follows:

$$\Delta x_{wi} = \frac{\Delta x_{i-1} + \Delta x_i}{2}, \quad \Delta x_{ei} = \frac{\Delta x_i + \Delta x_{i+1}}{2}. \tag{6}$$

Specially, for the beginning subdomain $i = n$ on the flux boundary and ending subdomain $i = 1$ on the boundary without flux, there are

$$\begin{cases} D_{en} \dfrac{M_{(n+1)} - M_n}{\Delta x_{en}} = S\left(M_{\text{eq}} - M_n\right), & \text{for } i = n \\ D_{w1} \dfrac{M_1 - M_{(0)}}{\Delta x_{w1}} = 0, & \text{for } i = 1. \end{cases} \tag{7}$$

Then, by grouping Eq 4 to Eq 6, Eq 5 can be re-written as the generic algebraic equation, see Eq 6:

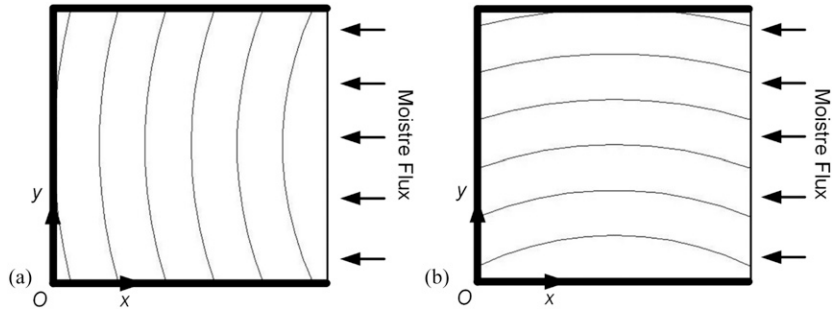

Figure 4. Geometrical configurations of (a) radial diffusion model and (b) tangential diffusion model used in numerical simulations.

$$a_{wi}M_{i-1} + a_iM_i + a_{ei}M_{i+1} = b_i. \tag{8}$$

The calculated formula of algebraic symbol in Eq 7 is given in Table 2.

Thus, by grouping equations described as aforementioned, the following equations system is shown in Eq 8:

$$\begin{bmatrix} a_1 & a_{e1} & & & & & \\ a_{w\ldots} & a_{\ldots} & a_{e\ldots} & & & & \\ & a_{w(i-1)} & a_{i-1} & a_{e(i-1)} & & & \\ & & a_{wi} & a_i & a_{ei} & & \\ & & & a_{w(i+1)} & a_{i+1} & a_{e(i+1)} & \\ & & & & a_{w\ldots} & a_{\ldots} & a_{e\ldots} \\ & & & & & a_{wn} & a_n \end{bmatrix} \begin{bmatrix} M_1 \\ M_{\ldots} \\ M_{i-1} \\ M_i \\ M_{i+1} \\ M_{\ldots} \\ M_n \end{bmatrix} = \begin{bmatrix} b_1 \\ b_{\ldots} \\ b_{i-1} \\ b_i \\ b_{i+1} \\ b_{\ldots} \\ b_n \end{bmatrix}. \tag{9}$$

Based on the tridiagonal matrix algorithm method, the EDC and SEC can be determined by solving Eq 8 as shown in Fig 3. In the flowchart, the relative error between the experimental and simulated data is used to determine the optimum values of the aforementioned parameters:

$$R = \frac{1}{n}\sum_{i=1}^{n}\left|\frac{M_{i\text{cal}} - M_{i\,\text{exp}}}{M_{i\,\text{exp}}}\right|, \tag{10}$$

where n is the number of slices, $M_{i\text{cal}}$ is the calculated MC of the ith slice in the algorithm, and $M_{i\,\text{exp}}$ is the experimental MC of the slice ith measured in the diffusion experiment.

Numerical Simulations

To analyze the orthotropic moisture diffusion behavior in wood, numerical simulations were conducted by the commercial finite element software COMSOL Multiphysics. The numerical experiments were performed on two Chinese fir 2D models with the size of 30×30 mm^2, and the moisture flux was conducted on the $x = 30$ mm boundary, see Fig 4.

Two numerical simulations, adsorption and desorption simulations, were performed on each Chinese fir model. The simulation sets are listed in Table 3. Material parameters of these models

Table 3. Parameters used for numerical experiments.

Parameters	Symbol	Adsorption simulation	Desorption simulation
Initial MC	M_0	0%	17.8%
Average transversal airflow	v	1.6 m/s	1.6 m/s
RH	M_{RH}	85 ± 5%	50 ± 5%
Equilibrium MC	M_{eq}	17.8%	9.1%
Temperature	T	25 ± 1°C	25 ± 1°C

Table 4. Measured results of parameters α, β, and S and mean relative errors on radial and tangential directions.

Parameters	Adsorption		Desorption	
	Radial	Tangential	Radial	Tangential
α	−21.01	−21.46	−20.87	−21.90
β	1.57	2.34	8.24	18.21
Surface emission coefficient ($m \cdot s^{-1}$)	8.83×10^{-8}	7.76×10^{-8}	3.44×10^{-7}	3.22×10^{-7}
$\bar{R}$	−1.19%	−3.74%	3.39%	3.38%

$\bar{R}$, mean relative error between measured and simulated results; P, P-value in significance analysis between radial and tangential diffusion curves.

were based on the results of EDC determination experiments.

RESULTS AND DISCUSSION

EDC and SEC Results

Experimental results of parameters α, β in Eq 2 and SEC on the radial and tangential directions are listed in Table 4. As shown in Table 4, regardless of adsorption or desorption processes, the values of SEC are still slightly lower in the radial direction. It can also be observed that SEC for adsorption process is significantly larger than SEC for desorption process.

Based on the test results of α and β, the values of EDC in the radial direction (D_R) and tangential direction (D_T) for Chinese fir at experimental MC from 9 to 18% are calculated and presented in Fig 5. It can be noted from Fig 5 that there is a remarkable difference of EDC in each direction. For the adsorption process, D_R is still larger than D_T, which is similar to SEC, and the increase rate of D_R is also slightly greater than D_T, whereas for the desorption process, the value of D_R becomes lower than tangential direction when MC is higher than 10%.

Moreover, comparing the experimental results between adsorption and desorption processes,

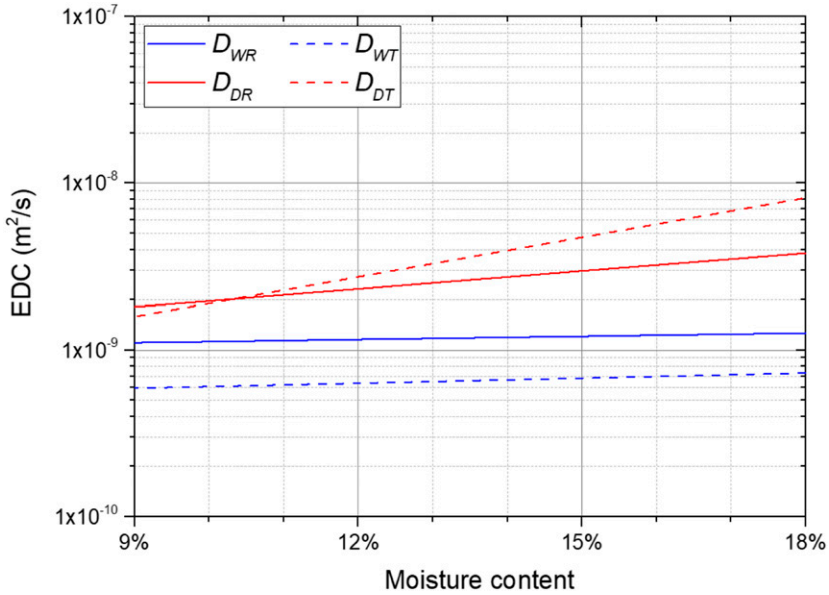

Figure 5. Effective diffusion coefficient under various MCs on radial (R) and tangential (T) directions in the adsorption and desorption experiments.

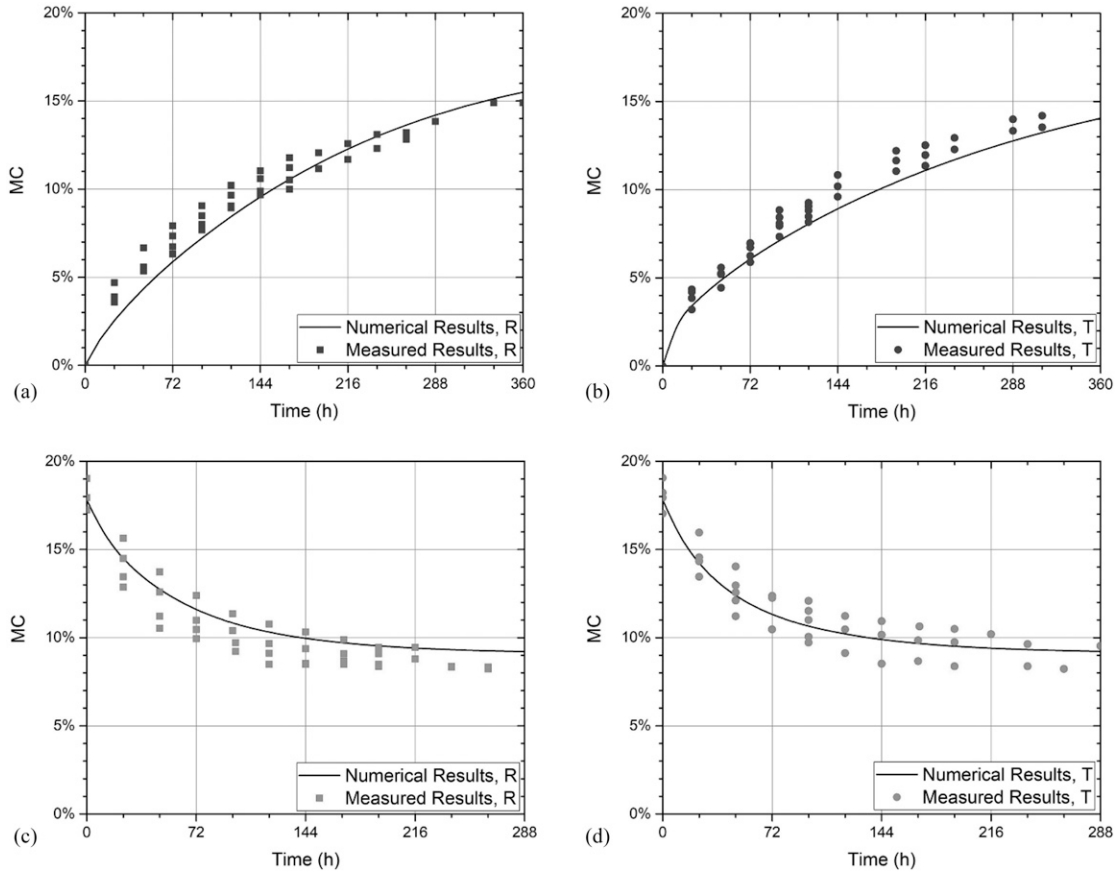

Figure 6. Absorbing and desorbing curves of experimental results and numerical results: (a) radial adsorption, (b) tangential adsorption, (c) radial desorption, and (d) tangential desorption.

the values are also different. The desorption process provides higher values of EDC than adsorption process at the specific MC in the experiments.

Numerical Simulations Results

Using experimental results of EDC and SEC, the one-dimensional diffusion curves of numerical simulations can be plotted, see Fig 6. The scatters are values of MC of each specimen which were recorded every 24 h before the specimen was sliced. As shown in Fig 6 and Table 5, there is a reasonable agreement between the simulated and experimental results for desorption and tangential adsorption experiments. Comparing the adsorption and desorption curves between radial and tangential diffusions, the *P*-value in significance analysis is far larger than 0.05 which means that the diffusion curves in the two directions are quite similar to each other. In the case of moisture adsorption, the time to steady state in the radial direction is shorter than that in the

Table 5. Time to steady state and statistical results of numerical simulations.

	Adsorption		Desorption	
Parameters	Radial	Tangential	Radial	Tangential
$\bar{R}$	−1.19%	−3.74%	3.39%	3.38%
t_s (d)	48	65	22	20
P	0.0878		0.9749	

$\bar{R}$, mean relative error between measured and simulated diffusion curves; t_s, time to steady state in numerical simulations; P, P-value in significance analysis between radial and tangential diffusion curves.

tangential direction, which behaves similar to the values of EDC and SEC, whereas for the moisture desorption process, the radial diffusion provides a slightly larger time to steady state regardless a higher value of SEC in this direction. This would indicate that the value of SEC appears to have little influence than EDC in the moisture diffusion model.

Figure 7 presents the MC distribution along the diffusion directions of each slice at different MC stages in the moisture diffusion experiments, where the scatters are the MC of each slices. As plotted in Fig 7, the accordance between simulation and experimental results is fairly good along the diffusion direction, although the experimental method for sectioning specimen slices may cause the MC of each slice to slightly decrease. The results suggest that the test results of the EDC and SEC yield good results for moisture adsorption and desorption process of wood.

CONCLUSION

In this article, the EDC and SEC of Chinese fir on radial and tangential directions during moisture adsorption and desorption process were studied by the diffusion model based on Fick's second law and the finite volume method. The results show that moisture transporting of Chinese fir behaves anisotropic on the radial and tangential directions. For adsorption process, the SEC and EDC of Chinese fir are all greater in the radial direction. For desorption process, the

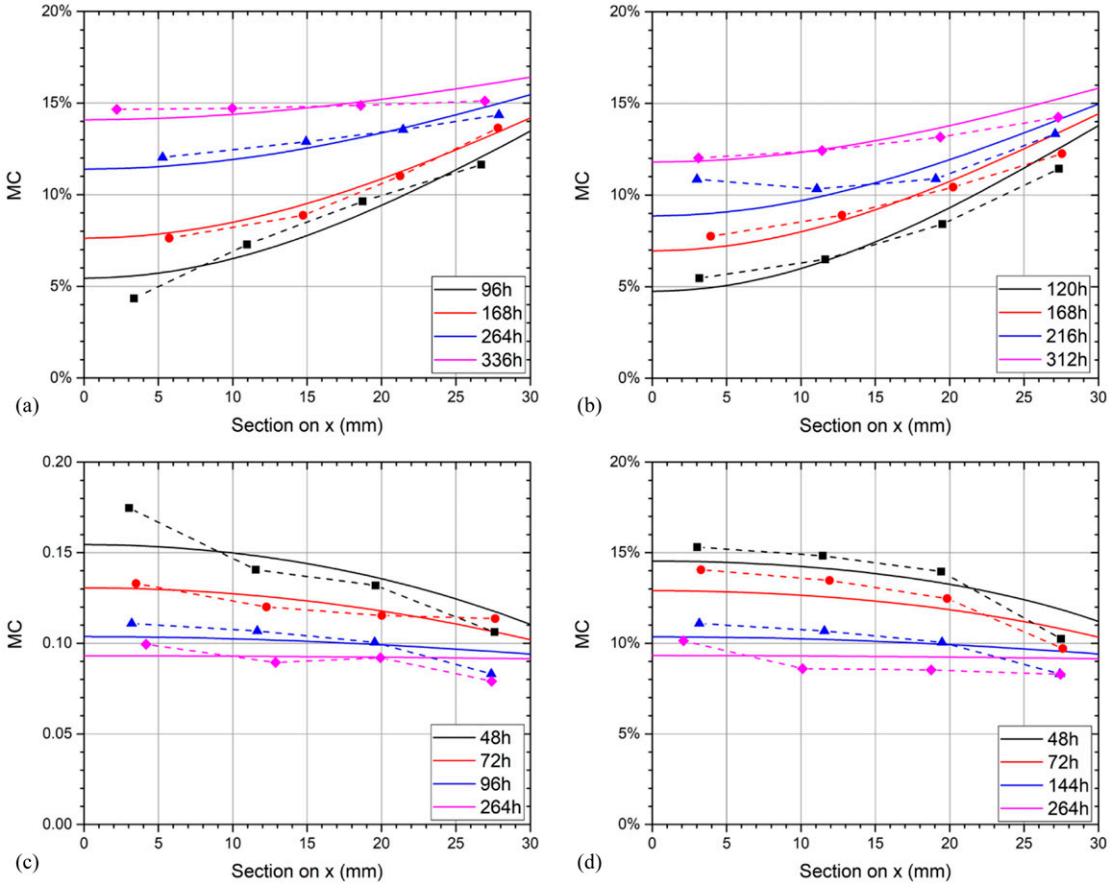

Figure 7. The measured and simulated MC distributions of Chinese fir along the diffusion directions: (a) radial adsorption, (b) tangential adsorption, (c) radial desorption, and (d) tangential desorption.

SEC is higher in the radial directions, whereas the EDC in the tangential direction is higher than that in the radial direction when the MC is greater than 10%.

Besides, the moisture diffusion parameters are also quite different between the adsorption and desorption processes. The values of EDC and SEC on the two directions are all larger in the adsorption process under the experimental MC (9-18%).

Then, numerical simulations of moisture diffusion on the two directions in Chinese fir were performed based on the parameters obtained from the diffusion experiments to determine the effectiveness of the diffusion parameters. The results show that the measured values of EDC and SEC of Chinese fir are capable to predict the development of MC and its distribution in Chinese fir during moisture diffusion processes. Although the diffusion curves behave quite similar in the two directions, the time to steady state is slightly shorter in the radial direction for adsorption process and in the tangential direction for desorption process.

ACKNOWLEDGMENT

The present research was supported by Beijing Natural Science Foundation (No. 2182045).

REFERENCES

Angst V, Malo KA (2012) The effect of climate variations on glulam–an experimental study. Eur J Wood Wood Prod 70: 603-613.

Angst V, Malo KA (2013) Moisture-induced stresses in glulam cross section during wetting exposures. Wood Sci Technol 47:227-241.

Chen Y, Choong ET, Wetzel DM (1996) A numerical analysis technique to evaluate the moisture-dependent diffusion coefficient on moisture movement during drying. Wood Fiber Sci 28(3):338-345.

Crank J (1975) The mathematics of diffusion, 2nd edition. Clarendon Press, Oxford, UK.

Eriksson J, Johansson H, Danvind J (2006) Numerical determination of diffusion coefficients in wood using data from CT-scanning. Wood Fiber Sci 38(2):334-344.

Gatica YA, Salinas CH, Ananias RA (2011) Modeling conventional one-dimensional drying of radiate pine based on the effective diffusion coefficient. Lat Am Appl Res 41: 183-189.

Gatica YA, Salinas CH, Ananias RA (2012) Modeling conventional two-dimensional drying of radiate pine based on the transversal effective diffusion coefficient. Lat Am Appl Res 42:381-388.

Hukka A (1999) The effective diffusion coefficient and mass transfer coefficient of Nordic softwoods as calculated from direct drying experiments. Holzforschung 53:534-540.

Jiang JL, Bachtiar EV, Lu JX, Niemz P (2017) Moisture-dependent orthotropic elasticity and strength properties of Chinese fir wood. Eur J Wood Wood Prod 75(6): 927-938.

Kaboorani A, Blanchet P, Laghdir A (2013) A rapid method to assess viscoelastic and mechanosorptive creep in wood. J Wood Sci 51(4):462-467.

Kollmann FP, Cote WA (1968) Principles of wood science and technology I: Solid wood. Springer-Verlag New York Inc., New York, NY.

Ma EN, Zhao GJ, Cao JZ (2005) Hygroexpansion of wood during moisture adsorption and desorption processes. For Stud China 7(2):43-46.

Nakano T (1995) Note on a formulation of a water adsorption process of wood. Wood Sci Technol 29:231-233.

Niklewski J, Fredriksson M, Isaksson T (2016) Moisture content prediction of rain-exposed wood: Test and evaluation of a simple numerical model for durability applications. Build Environ 97:126-136.

Roszyk E, Mania P, Molinski W (2012) The influence of micro fibril angle on creep of Scotch pine wood under tensile stress along the grains. Wood Res 57(3):347-358.

Salinas C, Chavez C, Ananias RA, Elustondo D (2015) Unidimensional simulation of drying stress in radiate pine wood. Dry Technol 33:996-1005.

Shi SQ (2007) Diffusion model based on Fick's second law for the moisture adsorption process in wood fiber-based composites: Is it suitable or not. Wood Sci Technol 41: 645-658.

Simpson WT (1974) Measuring dependence of diffusion coefficient of wood on moisture concentration by adsorption experiments. Wood Fiber Sci 5(4):299-307.

Skaar C (1988) Wood-water relations. Springer-Verlag, Berlin, Heidelberg, Germany.

Sundström T, Kevarinmäki A, Fortino S, Toratti T (2011) Shear resistance of glulam beams under varying humidity conditions. VTT Technical Research Centre of Finland Ltd, Finland.

Tsuchikawa S, Siesler H (2003a) Near-infrared spectroscopic monitoring of the diffusion process of deuterium-labeled molecules in wood part I: Softwood. Appl Spectrosc 57(6): 667-674.

Tsuchikawa S, Siesler H (2003b) Near-infrared spectroscopic monitoring of the diffusion process of deuterium-labeled

molecules in wood part II: Hardwood. Appl Spectrosc 57(6):675-681.

United States Department of Agriculture (2010) Wood Handbook: Wood as an Engineering Material. United States Department of Agriculture Forest Service, Madison, WI.

Wadso L (1993) Measurements of water vapor sorption in wood: Part 2. Results. Wood Sci Technol 28:59-65.

Willems W (2014) The water vapor sorption mechanism and its hysteresis in wood: The water/void mixture postulate. Wood Sci Technol 48:499-518.

Yeo H, Eom CD, Han Y, Kang W, Smith WB (2008) Determination of internal moisture transport and surface emission coefficients for eastern white pine. Wood Fiber Sci 40(4):553-561.

Zhan TY, Jiang JL, Lu JX, Peng H (2015) Dynamic viscoelastic properties of Chinese fir under cyclical relative humidity variation. J Wood Sci 61(5):465-473.

Zhao YK, Iida I, Feng SH, Lu JX (2012) Viscoelastic properties of wood from Chinese-fir and polar plantations. For Stud China 14(2):107-111.